Hollow Cathode Micro-Thruster Performance*†

Michael J. Patterson and John E. Foster
National Aeronautics and Space Administration
Glenn Research Center
MS 301-3
21000 Brookpark Road
Cleveland, Ohio 44135
216-977-7481
Michael.J.Patterson@grc.nasa.gov

IEPC-01-226

The NASA Glenn Research Center ion propulsion program addresses the need for high specific impulse ion propulsion systems and technology across a broad range of mission applications and power levels, including evaluation of micro-ion propulsion concepts. An effort was undertaken to evaluate the feasibility of developing a "micro" ion thruster based on a small hollow cathode, with an overall performance exceeding 25% efficiency at > 1500 seconds specific impulse, operating at input power levels up to about 50 W. A laboratory investigation was undertaken to examine the basic physics controlling ionization processes of small, low power hollow cathodes. Controlling design parameters were identified, and high-efficiency (3 50% ionization efficiency) hollow cathodes were fabricated. A prototype hollow cathode micro-thruster was fabricated and performance characterized with high-voltage beam extraction up to 1500 V.

Introduction

With the success of the NASA Solar Electric Propulsion Technology Applications Readiness program ion propulsion system on the Deep Space One spacecraft,[1] the future for this propulsion technology for other NASA missions appears promising. Potential applications for ion propulsion include micro-spacecraft. As an example, a general need for high specific impulse (> 1000 sec), low-power (~10 W) propulsion has been identified for second generation Jet Propulsion Laboratory (JPL) micro-spacecraft[2] and there is the potential for micro-ion propulsion concepts to play a role. An engine with these characteristics fills the gap between micro Newton concepts and ~100 W class electric propulsion thrusters, with the potential for use on a variety of micro-spacecraft for primary propulsion, station keeping, and formation flying.

At NASA Glenn Research Center (GRC), considerable work has been conducted in the development of small (3.2 mm diameter) hollow cathode technology for electric propulsion. In-house a number of designs have been manufactured and characterized, and tests have been conducted to parametrically assess the impact of design parameters on cathode efficiency.[3,4] This work has been complemented by a contracted effort to apply newly-developed computer models of hollow cathode operation to understand the mechanisms controlling ion generation in the cathode orifice,[5] and a university experimental effort to investigate plasma processes.[6]

*Presented as Paper IEPC-01-226 at the 27th International Electric Propulsion Conference, Pasadena, CA, 15-19 October, 2001.

The results of these experiments and modeling indicated that hollow cathodes could, under certain regimes, ionize a high fraction of propellant at relatively low power levels. Substantial ionization occurs within the cathode orifice; the conditions at the cathode orifice yielding the highest current density, the most ohmic heating, and a high neutral density. These results were collaborated elsewhere using similar experimental hardware.[7]

If hollow cathodes can be constructed to yield high ionization efficiencies, then there is the potential for developing a simple and efficient low-thrust propulsion device using them. The device, referred to as a Hollow Cathode Micro-Thruster (HCMT), would provide thrust by accelerating ions (produced by the hollow cathode) utilizing a high-voltage acceleration stage. The HCMT is shown conceptually in Figure 1.

The basic principles of HCMT operation would involve:

- generation of ion current from an optimized hollow cathode;
- expansion of the ions with minimal-loss, using electrostatic reflection;
- acceleration of the ions using a small diameter ion optics system;
- beam neutralization using field emitter array cathode technology (or other efficient means); and
- thrust vectoring using electrostatic deflection.

The proposed HCMT overcomes difficulties preventing scaling down conventional ion engines and Hall thrusters because the ionization process eliminates the issues associated with neutral loss and magnetic confinement. Using the ions from the hollow cathode directly eliminates the need for a separate discharge (ionization) chamber and associated power supply, and magnetic field, as compared with typical methods of ion production. The low ion beam current (~10 mA) produced would permit the use of simpler neutralization schemes than implemented on conventional ion engines.

An activity was initiated to evaluate the feasibility of various micro ion propulsion concepts. The goal is to develop an engine with >25% efficient, ≥1500 seconds specific impulse, at ≤50 W input power. While issues of system specific mass (including power electronics) and propellant management may eventually conspire to preclude development of a competitive propulsive concept, an investigation of this type clarifies the operational limits and provides impetus for understanding. One such concept under investigation is the HCMT. This paper discusses the performance of the hollow cathode discharge, and the performance of a laboratory model HCMT with high-voltage beam extraction.

Test Support Equipment

Facility

Testing was performed in NASA GRC's Vacuum Facility 52, shown in Figure 2. The facility is a 0.61-m diameter by 0.91-m long stainless steel bell jar with a 0.25-m helium cryopump with a pumping speed of 4000 liters per second (nitrogen).

Diagnostics

The vacuum facility had a 2-D motion control system, with one stage capable of 408 mm of axial translation and a transverse stage capable of 208 mm of radial translation. A Faraday probe diagnostic was mounted atop the motion control system for plume interrogation.

Two Faraday probes of different diameters were used in this investigation. The two probes measured 1.5 mm and 3.2 mm in diameter. Two different probe sizes were used to investigate two effects: probe perturbation of the operation of the thruster; and finite surface area error effects because probe is not a point collector. The probes were biased –25 V with respect to facility ground to repel plasma electrons. An electrometer was used to bias and measure current collected by the probes as they were swept across the engine ion beam. The ion beam current was calculated from the acquired profiles by integration. The curves were integrated assuming the beam profiles were symmetrical. To first order, this requirement was satisfied as the profiles acquired were nearly Gaussian in shape. Discrepancies between metered beam current and integrated probe values were attributed to collection of background plasma and finite probe surface area.

The Faraday probe was also used as a floating potential diagnostics. In this capacity, the probe was used to determine the floating potential downstream of the engine. This data was used to assess the degree of neutralization in the plume.

Power Supplies
Test and evaluation of the HCMT discharge, and with beam extraction, were conducted using commercial power supplies configured into a console. The console included analog circuitry to control high-voltage arcing that may occur between the electrodes of the ion optics, or between the engine high voltage surfaces and facility ground.

The electrical configuration is shown in Figure 3. As indicated, the positive voltage output of the discharge power supply was electrically tied to the positive voltage output of the beam power supply. Also, the common tie-point of the negative voltage output of the beam power supply and the positive voltage output of the accelerator power supply was attached to facility ground; beam neutralization during beam extraction was accomplished via the vacuum facility walls.

The HCMT was operated with a total of 3 power supplies during beam extraction and these included discharge, beam, and accelerator power supplies. A heater supply was used to facilitate discharge ignition. The HCMT discharge was characterized over a cathode emission current range of approximately 0.5A to 2.0 A, and from 2.0-2.5 A with beam extraction. During beam extraction, the beam power supply voltages ranged from about 560-1750 V, while the accelerator power supply voltage was operated between -150 V and -180 V.

Propellant Feed
All testing was performed using research grade xenon gas. Selection of xenon was in part motivated by the fact that all recent development work on 3.2 mm cathode technology had used xenon. It is an attractive propellant of choice for conventional ion propulsion because of its high atomic mass, low ionization potential, it is non-reactive and non-contaminating, and it has excellent storage properties. It is not clear however that this, or other inert gases, would necessarily be the ideal propellant choice for a micro ion engine; liquid metal propellants for example may be more appropriate.

A xenon gas feed system was designed and constructed for performance assessments of the HCMT. The feed system minimizes contaminants in the gas supply by using high purity xenon and by using construction techniques which limit the introduction of contaminants into the gas stream. The feed system contains a single propellant line delivery to the HCMT, using a 5.0 sccm full-scale commercial mass flow controller (MFC) to control the propellant flow. The MFC, calibrated using a secondary standard, was capable of controlling the propellant flow rate to within 0.05 sccm (1% of full-scale).

Hollow Cathode Micro-Thruster

The laboratory model HCMT consists of a hollow cathode (internal to the discharge), a discharge chamber, and a 2-grid ion optics assembly, all contained within a plasma screen to shield engine high-voltage surfaces from the surrounding plasma. Upstream of the hollow cathode are a series of commercial cryogenic breaks used to electrically isolate the engine from the xenon propellant feed system. During operation with beam extraction, beam neutralization was accomplished via electron emission from the vacuum facility walls.

Cathode
The hollow cathode was constructed from a refractory alloy tube of 3.2 mm diameter. The orifice plate at the end of the tube was secured via electron beam welding. The orifice plate geometry (orifice diameter, and aspect ratio of the orifice) was selected after a number of designs were evaluated experimentally, and numerically, with the objective of creating a design which maximized hollow cathode ion production and ion transmission. The orifice plate surface has or convex configuration to reduce ion recombination losses which could occur on forward surfaces of the plate due to ion plume expansion.

Contained within the tube is an electron emitter consisting of a porous tungsten cylinder impregnated with a low-work function compound. External to the hollow cathode tube is a swaged heater cable used to elevate the electron emitter to thermionic temperatures during ignition. During operation, the cathode is self-heating, and the heater is thus de-energized.

Discharge
The discharge chamber was fabricated from aluminum and is conic in shape, with an axial length of about 1.5 cm, and forward (beam) diameter of approximately 4.9 cm, yielding an expansion angle of approximately 55 degree. The shape was determined computationally to

maximize the transmission of ions produced in the throat of the hollow cathode. The surface of the discharge chamber is at anode potential, and thus collects the cathode emission current. There is no applied magnetic field.

In effect, the discharge chamber simply acts as an electrode for electron current collection, and as a structural element to mechanically support and locate the ion optics with respect to the hollow cathode. This is a departure from convention ion engines in which the discharge chamber functions to contain the neutral propellant, and increase the residence time and ionization efficiency of high energy electrons from the hollow cathode. With the small dimensions of the HCMT discharge, there is negligible impact ionization in the discharge; ion production is assumed to occur entirely within the throat of the hollow cathode orifice.

Ion Optics

The electrodes for the HCMT ion optics were fabricated from pre-existing concave electrodes originally manufactured for an 8-cm beam diameter ion engine, but with a diameter reduced to about 4.8 cm. The ion optics consisted of 2 electrodes (screen and accelerator grids) made of molybdenum, with the assembly aligned and gapped using boron nitride spacers. The geometry of the screen grid had a thickness of approximately 0.38 mm, with 1.91 mm diameter circular apertures in a hexagonal array creating an effective open-area-fraction of about 67%. The accelerator grid was approximately 0.51 mm thick, with 1.14 mm circular apertures in a hexagonal array creating an open-area-fraction of about 24%. The grid-to-grid spacing was set to approximately 1.0 mm. The screen grid was electrically-tied to cathode common potential, and isolated from the downstream surface of the discharge chamber using an isomica insulator.

Results and Discussion

This section discusses the performance of the cathode, the discharge operation including ionization efficiency, and operation of the HCMT with beam extraction.

Cathode and Discharge

The hollow cathode ignited and operated stably over the range of emission currents (0.5-2.5 A from hollow cathode to anode) and xenon flow rates (0.5-3.0 sccm) investigated. Typical anode voltages varied from about 14-44 volts. For these experiments, a swaged heater was used to condition, and facilitate ignition of the cathode. Typical ignition times, from application of heater power to the cathode, were of the order of 2 minutes. In a higher-fidelity HCMT, the heater would be eliminated in favor of using a high-voltage pulse ignitor to simplify engine operation.

The discharge was operated without the ion optics assembly for these tests. This configuration is shown in Figure 4. This was done so that the low-energy ion efflux at the exit plane of the discharge chamber could be characterized. During parametric operation of the discharge, as both the xenon propellant flow rate (through the hollow cathode) and the cathode emission current were varied, the ion efflux was measured across the exit plane of the discharge 1 mm downstream using the Faraday probe. Peak current density and integrated total ion current values were obtained at each operating condition to assess the ionization fraction. A typical profile of the ion plume from the discharge is shown in Figure 5. The discharge conditions were 0.5 A cathode emission current, and 1.0 sccm flow rate. The peak current density was about 3.3×10^{-4} A/cm^2.

Figure 6 shows the anode voltage versus cathode emission current for several xenon flow rates. In general, the anode voltage decreased with increasing emission current and flow rate. The discharge operated at anode voltages less than about 21 volts for xenon flow rates $\geq$ 2.0 sccm at all emission currents. The anode voltage was less than 25 volts for flow rates $\leq$ 1.0 sccm, above about 1.0 amperes emission.

Figure 7 displays the total ion current measured exiting the discharge as a function of xenon flow rates, for various values of cathode emission current. As indicated, the total ion current in general increased with increasing flow rate, at a fixed emission current. For example, at 1.0 A cathode emission current, the total ion current increased from about 7.5 mA to 14.9 mA going from 1.0 to 3.0 sccm. Similar behavior was observed at 1.5 and 2.0 amperes. At 0.5 A, the ion current produced saturated at a value of about 5.1-5.2 mA for flow rates above 2.0 sccm.

Also from Figure 7, the total ion current produced

increased approximately linearly with increasing cathode emission current, at a given flow rate. At 1.0 sccm xenon flow, the ion current increased from about 3.5 mA to 19.8 mA, as the cathode emission current increased from 0.5 to 2.0 amperes. The maximum ion production occurred at the highest combination of xenon flow rate and emission current; 19.8 mA at 1.0 sccm and 2.0 amperes. The anode voltage and discharge power at this condition was 18.3 V and 36.6 W respectively.

Although the ion current produced increases with total flow rate at fixed emission current, the ionization fraction decreases, as illustrated in Figure 8. Figure 8 shows the ionization fraction (as defined by the ratio of the total integrated ion current to flow rate into the hollow cathode in equivalent milliamperes) versus flow rate for various values of cathode emission current. As indicated, the maximum ionization fraction occurs at the combination of highest cathode emission current and lowest xenon flow rate. For the conditions shown in Figure 8, the maximum ionization fraction was approximately 0.51, at 2.0 amperes emission current and 0.5 sccm flow. The anode voltage and discharge power at this condition was 15.9 V and 31.8 W respectively. This ionization fraction is typically about one order-of-magnitude higher than observed using conventional 6.4 mm diameter hollow cathode technology in ion engine discharges. At higher flow rates, the ionization fraction drops off precipitously.

Figure 9 is a plot of discharge losses (Watts of discharge power per milliampere of ion current) versus ionization fraction for different cathode emission currents. The discharge losses are typically about one order-of-magnitude higher than those observed in conventional ion engine discharge chambers with ion beam extraction. They range for the HCMT from a low of about 1.1 W/mA at 1.5 A emission current and 0.09 ionization fraction, to in-excess-of 6.8 W/mA at 0.5 A emission current and 0.05 ionization fraction. At 2.0 A emission current the discharge losses were fairly constant at about 1.7-1.9 W/mA over 0.27-0.51 ionization fraction.

Beam Extraction

Subsequent to discharge characterization, the ion optics assembly was installed on the discharge chamber and the entire HCMT was enclosed in a plasma screen. The HCMT was then operated with beam extraction. For these tests, the discharge was operated at 2.0 amperes cathode emission current, between 0.5-1.0 sccm xenon flow rate. These values correspond to the conditions yielding the highest discharge ionization efficiency during tests without beam extraction.

Beam extraction and stable operation of the HCMT was achieved over a range of beam power supply voltages; from about 560 to 1750 V. The corresponding accelerator grid voltages ranged from about –150 to –180 V. Figure 10 shows the HCMT and collimated ion beam during operation. The accelerator drain current was typically high; about 0.35-0.70 of the beam current. This is likely due to a combination of direct ion impingement, and facility-enhanced charge-exchange ion current. The facility pressure was typically in the range of $1.6\text{-}3.7 \times 10^{-3}$ Pascals ($1.2\text{-}2.8 \times 10^{-5}$ Torr).

With beam extraction, the magnitude of the metered beam current (the difference between the beam power supply current and the accelerator power supply current), and the magnitude of the integrated Faraday probe current were both considerably lower than the values measured downstream of the open-ended anode during discharge tests. As an example, the metered beam current at 2.0 cathode emission current and 0.75 sccm xenon flow rate was of the order of 7.5-7.7 mA with beam extraction, compared to about 18.8 mA during discharge testing, even though the discharge input power was similar in both circumstances.

This reduction in current is likely associated with ion recombination losses on the surface of the screen grid and direct ion impingement on the accelerator grid. It is speculated that because of the relatively high kinetic energy ions emitted from the hollow cathode, the electrostatic focussing of the ion optics is low which reduces the effective ion transparency. Typical ion optics of comparable electrode design implemented on large-area conventional engines have an electrostatic transparency of about 0.80; the optics on the HCMT were apparently operating at about 0.40 transparency. This may have been exacerbated by the large grid-to-grid gap (1.0 mm) which was about 54% larger than typically employed. Some direct impingement on the accelerator grid was evident during examination after completion of testing.

Figure 11 shows the discharge losses versus onization

fraction both with and without beam extraction, at 2.0 A cathode emission current. In the beam extraction case, the ion current used was that measured from power supply instrumentation; in the discharge case, the ion current was that measured from the integrated Faraday probe trace obtained at the exit plane of the discharge. With beam extraction the ionization fraction was only of the order of 0.10-0.14, at discharge losses of 3.7-4.3 W/mA.

The overall engine performance parameters (neglecting neutralizer power) can be computed from the measured current, voltage, and flow rate instrumentation. The engine thrust can be calculated from:

$$F = g \cdot (2\frac{m}{q})^{1/2} \cdot J_b \cdot (V_b)^{1/2}$$

where g is a total thrust-loss correction factor, m is the ion mass, q is the ion charge, J_b is the ion beam current, and V_b is the beam voltage. The total thrust-loss correction factor, g, includes a factor for doubly-charged ions, and for off-axis beamlet vectoring.[8] The ion beam current, J_b, was obtained from the difference between the metered beam power supply current and the accelerator power supply current. The beam voltage, V_b, under this test condition is equivalent to the beam power supply voltage.

The specific impulse can be calculated from:

$$I_{sp} = h_u \cdot g \cdot (2q\frac{V_b}{m})^{1/2} \cdot \frac{1}{g}$$

where h_u is the propellant efficiency, which is the ratio of the beam current to the total propellant flow rate, and g is acceleration due to gravity. For the HCMT, the total propellant flow rate includes the xenon flow through the hollow cathode, plus an additional term to account for propellant flow ingested from the facility back into the discharge chamber through the ion optics.[8]

The input power can be calculated from:

$$P_{in} = (V_{bps} \cdot I_{bps}) + (V_{anode} \cdot I_{anode}) + (I_{accel} \cdot |V_{accel}|)$$

where V_{bps} and I_{bps} are the voltage and current of the beam power supply, V_{anode} and I_{anode} are the voltage and current of the discharge power supply, and V_{accel} and I_{accel} are the voltage and current of the accelerator power supply.

The total HCMT efficiency is then given by:

$$h_{HCMT} = \frac{F \cdot I_{sp} \cdot g}{2 \cdot P_{in}}$$

Overall performance numbers for the HCMT were calculated for two operating conditions which yielded the lowest discharges losses and highest ionization fraction, corresponding to a cathode emission current of 2.0 A, a flow rate of 0.75 sccm, at 1100 V and 1500 V beam power supply voltages. The data are shown in Table I.

Table I

V_b, V	F, mN	I_{sp}, sec	P_{in}, W	h_{HCMT}
1100	0.37	506	48.3	0.018
1500	0.42	569	51.6	0.022

As indicated, the overall engine efficiency is extremely low. This is due to a combination of low propellant efficiency (approximately 0.14) and high discharge losses (4.2-4.3 W/mA). At the 1500 V beam voltage condition, 61% of the input power is going into the discharge. Had the propellant efficiency been 0.35 (18.8 mA beam current) as measured prior to installation of the ion optics at this emission current and flow rate, the I_{sp} would be 1556 sec, with an efficiency of 0.12.

Figure 12 plots the peak ion current density of the ion beam versus radial position, for several axial distances downstream of the accelerator grid. The HCMT was operating at 1100 V beam voltage, 2.0 A cathode emission current, and 1.0 sccm, with a metered beam current of about 9.2 mA. The peak current density at 14 mm was about 1.3×10^{-3} A/cm^2, and drops off to about 8.0×10^{-4} A/cm^2 at 54 mm. The profiles indicate that the peak current density is skewed off of the geometric centerline of the engine; this is likely attributable to a misalignment in the hollow cathode with respect to the axis of the discharge and the center of the ion optics. The beam flatness parameter, the ratio of peak-to-average current density, for the 14 mm profile is about 0.53, which is typical of conventional ion engines.

Floating potential measurements were also obtained using the Faraday probe. For the 1100 V beam voltage condition identified in Table I (J_b of 7.74 mA), the potential was about 46 volts 15 mm downstream of the accelerator grid on-axis; high, likely due to the use of the vacuum chamber wall downstream as a source of

neutralizing electrons. The potential dropped to about 18 volts 215 mm downstream.

It is of value to calculate the propellant efficiencies and maximum acceptable discharge losses that are required of the HCMT to yield at least a 25% engine efficiency, at ≥1500 seconds I_{sp} and ≤50 W P_{in}, Assuming a g of 0.96, a J_a/J_b of 0.25%, a beam current of 7.74 mA, and neglecting neutralizer losses, propellant efficiencies and corresponding maximum acceptable discharge losses (ε_I) are given in Table II which yield 25% engine efficiency, for various beam voltages.

Table II $h_{HCMT} = 0.25$

h_u	Max ε_I, W/mA	I_{sp}, sec	P_{in}, W
1500 V V_b, 0.48 mN thrust			
1.00	4.010	4575	42.7
0.90	3.452	4118	38.3
0.80	2.915	3660	34.1
0.70	2.357	3203	29.9
0.60	1.798	2745	25.5
0.50	1.261	2288	21.3
0.40	0.703	1830	27.1
0.33	0.310	**1501**	14.0
2000 V V_b, 0.55 mN thrust			
0.90	4.610	4755	**51.2**
0.80	3.866	4226	45.4
0.70	3.142	3698	39.8
0.60	2.398	3170	34.0
0.50	1.674	2641	28.4
0.40	0.951	2113	22.8
0.30	0.207	**1585**	17.1
2500 V V_b, 0.61 mN thrust			
0.70	3.928	4135	**49.8**
0.60	2.997	3544	42.6
0.50	2.067	2953	35.4
0.40	1.158	2363	28.3
0.30	0.248	**1772**	21.3

These data are also shown in Figure 13, a plot of maximum acceptable discharge losses versus beam ionization fraction for various beam voltages. As noted, as the beam voltage increases, the acceptable discharge losses increase for a fixed propellant efficiency, to yield 25% engine efficiency. This is because the fraction of power that is going into the ion beam is increasing.

Also plotted in Figure 13 are the data obtained from the operation of the HCMT discharge prior to installation of the ion optics. As illustrated in Figure 13, if the discharge performance documented (0.50 ionization fraction at about 1.8 W/mA) in Figure 11 could be replicated with beam extraction, the overall engine efficiency would be ≥25% for beam voltages ≥2000 V.

One may conclude that the electrical and propellant efficiencies of the hollow cathode are sufficient to achieve the performance goals, for beam voltages in excess of 2000 V. However design modifications to the ion optics will be required to improve the ion transparency. Sufficient ions are being created, but insufficient numbers are being extracted into the ion beam. Optimization of the ion optics design may require quantifying the energies and trajectories of the ions from the hollow cathode.

Conclusions

An activity has been initiated at NASA GRC to evaluate the feasibility of various micro ion propulsion concepts. The goal is to develop an engine with >25% efficient, ≥1500 seconds specific impulse, at ≤50 W input power. One device under investigation is the Hollow Cathode Micro-Thruster (HCMT), which provides thrust by the electrostatic acceleration of ions produced by a hollow cathode.

A laboratory model HCMT was fabricated and tested. Critical design parameters of the hollow cathode were determined after a number of designs were evaluated, with the objective of maximizing ion production and ion transmission.

The discharge was operated initially without the ion optics so that the low-energy ion efflux at the exit plane of the discharge chamber could be characterized. Peak current density and integrated total ion current values were obtained at a variety of conditions. The anode voltage decreased with increasing emission current and flow rate. The discharge operated at anode voltages less than about 21 volts for xenon flow rates ≥ 2.0 sccm at all emission currents, and less than 25 volts for flow rates ≤ 1.0 sccm, above about 1.0 amperes emission.

The total ion current produced by the hollow cathode in general increased with increasing flow rate, at a fixed emission current. Although the ion current produced increased with total flow rate at fixed emission current, the ionization fraction decreased. The total ion current also increased approximately linearly with increasing cathode emission current, at a given flow rate.

The maximum ion production occurred at the highest combination of xenon flow rate and emission current; 19.8 mA at 1.0 sccm and 2.0 amperes. The maximum ionization fraction occurred at the combination of highest cathode emission current and lowest xenon flow rate; approximately 0.51, at 2.0 amperes emission current and 0.5 sccm flow.

The hollow cathode ionization fraction is typically about one order-of-magnitude higher than observed using conventional hollow cathode technology in ion engine discharges. The discharge losses are also typically about one order-of-magnitude higher than those observed in conventional ion engine discharge chambers with ion beam extraction. At 2.0 A emission current the discharge losses were fairly constant at about 1.7-1.9 W/mA over 0.27-0.51 ionization fraction.

Beam extraction was achieved over a range of beam power supply voltages. With beam extraction, the magnitude of the beam current was considerably lower than the values measured downstream of the open-ended anode during discharge tests. The reduction in current is likely associated with ion recombination losses and direct impingement on the ion optics assembly. With beam extraction the beam ionization fraction was only 0.10-0.14, at discharge losses of 3.7-4.3 W/mA, which resulted in very low engine efficiencies. However, if the discharge performance documented could be replicated with beam extraction, the overall engine efficiency would be ≥25% for beam voltages ≥2000 V.

The electrical and propellant efficiencies of the hollow cathode are sufficient to achieve the performance goals for beam voltages in excess of 2000 V. However design modifications to the ion optics will be required to improve the ion transparency. Current density plots of the ion beam were documented as well, indicating a beam flatness parameter of about 0.53, which is typical of conventional ion engines.

References

[1] Polk, J.E., et al., "Validation of the NSTAR Ion Propulsion System On the Deep Space One Mission: Overview and Initial Results," AIAA Paper No. 99-2274, June 1999.

[2] Sercel, J., "Representative Mission Requirements for Micropropulsion Systems," presentation at the JPL Micropropulsion Workshop, April 1997.

[3] Patterson, M.J., "Low-Power Ion Thruster Development Status," AIAA Paper No. 98-3347, July 1998.

[4] Patterson, M.J., et al., "Recent Development Activities in Hollow Cathode Technology," Paper No. IEPC-01-270. Proposed for presentation at the International Electric Propulsion Conference, October 2001.

[5] Katz, I., et al., "Sensitivity of Hollow Cathode Performance to Design and Operating Parameters," AIAA Paper No. 99-2574, June 1999.

[6] Domonkos, M.T., et al., "Low-Current Hollow Cathode Operation," AIAA Paper No. 99-2575, June 1999.

[7] Crofton, M.W., "Preliminary Mass Spectrometry of a Xenon Hollow Cathode," *Journal of Propulsion*, Volume 16, No. 1, pp. 157-159.

[8] Patterson, M.J., "Low-Isp Derated Ion Thruster Operation," AIAA Paper No. 92-3203, July 1992.

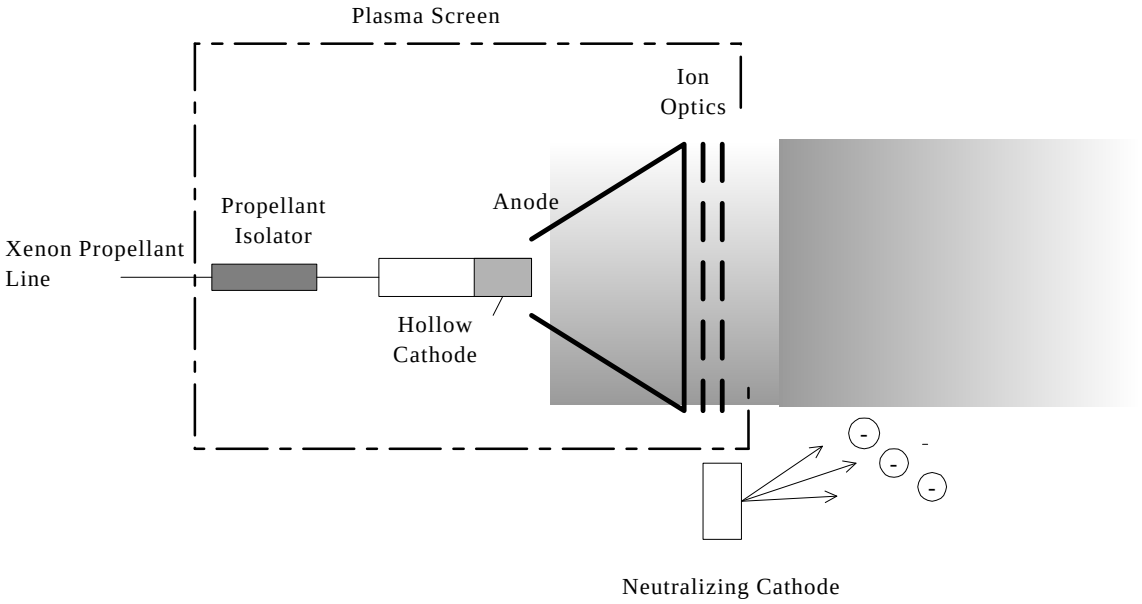

Figure 1 – Conceptual design of the HCMT.

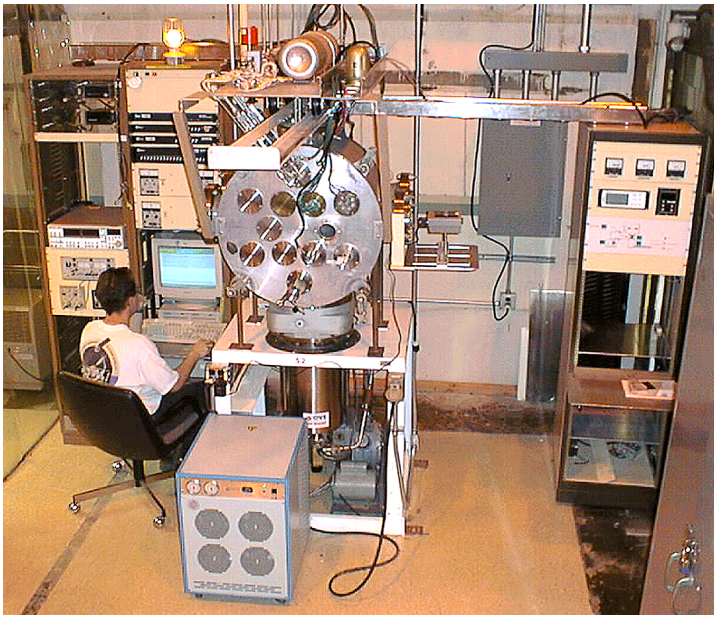

Figure 2 – Vacuum facility for HCMT testing.

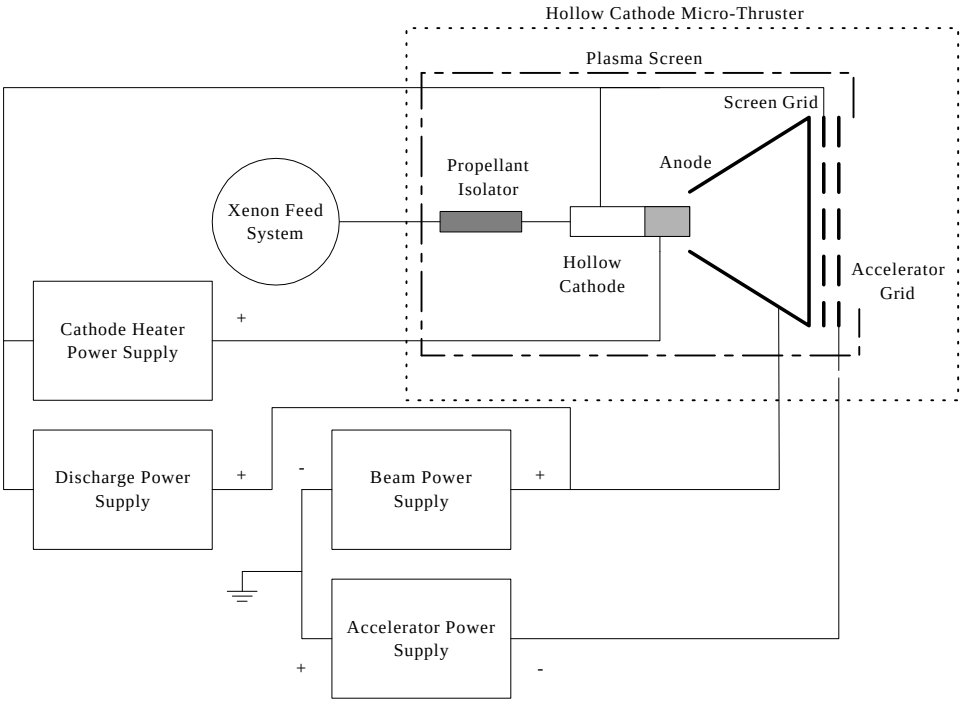

Figure 3 – Electrical test configuration.

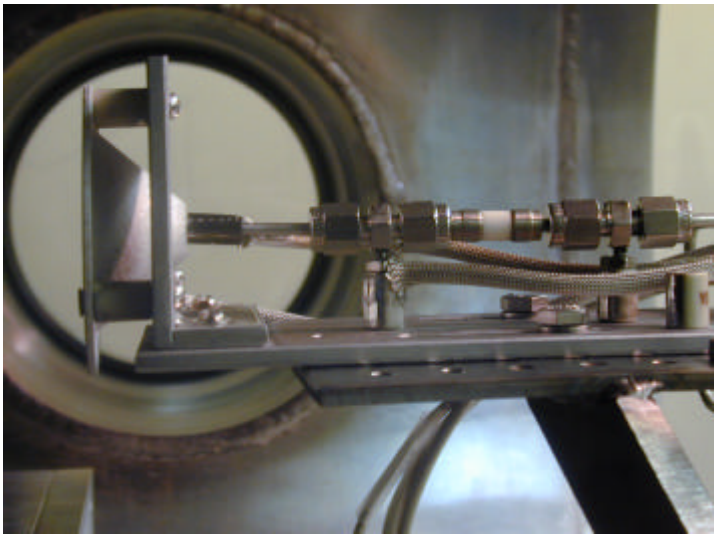

Figure 4 – HCMT, less ion optics and plasma screen.

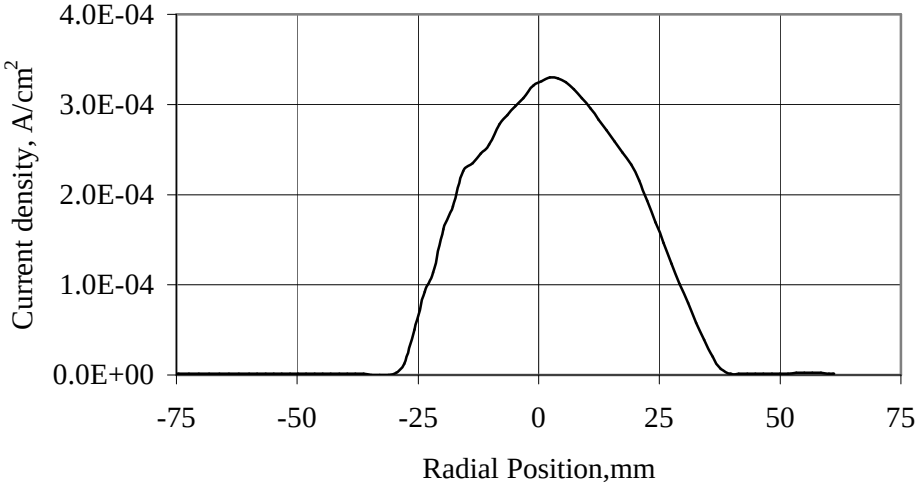

Figure 5 - Ion current density profile from discharge, 1 mm downstream; 0.5 A cathode emission current, 1.0 sccm xenon flow rate. Ion optics removed.

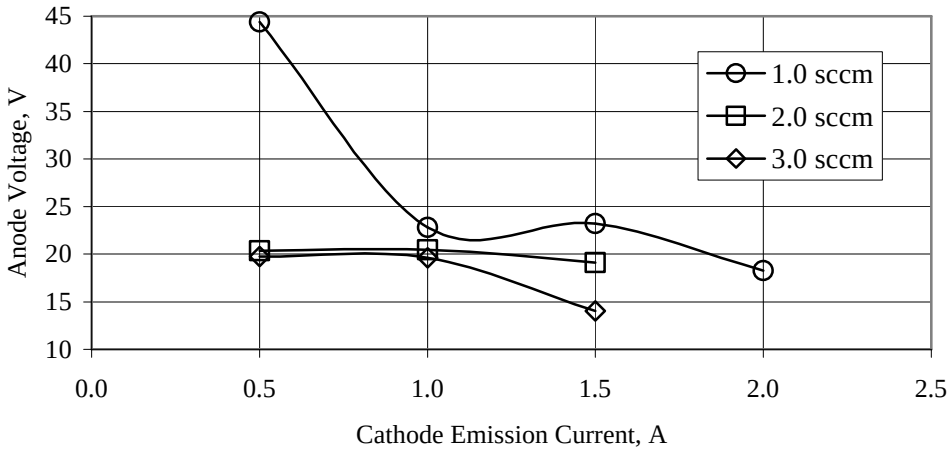

Figure 6 - Anode voltage versus cathode emission current for various xenon flow rates. Ion optics removed.

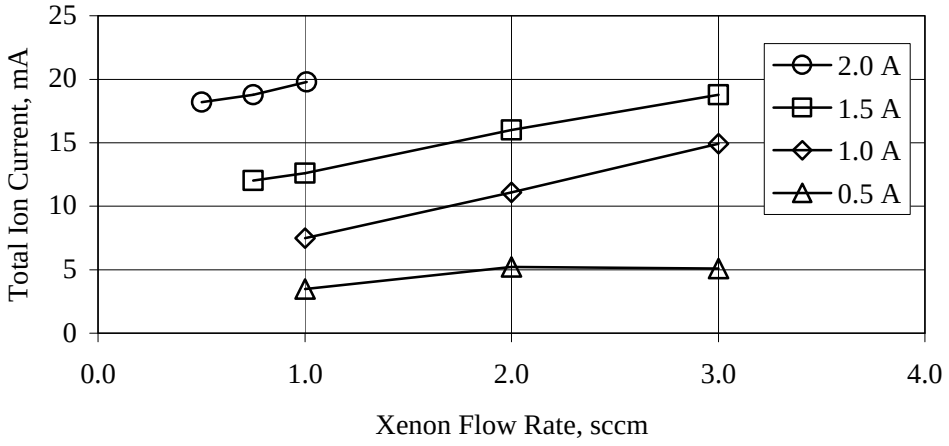

Figure 7 - Total ion current versus xenon flow rate for various cathode emission currents. Ion optics removed.

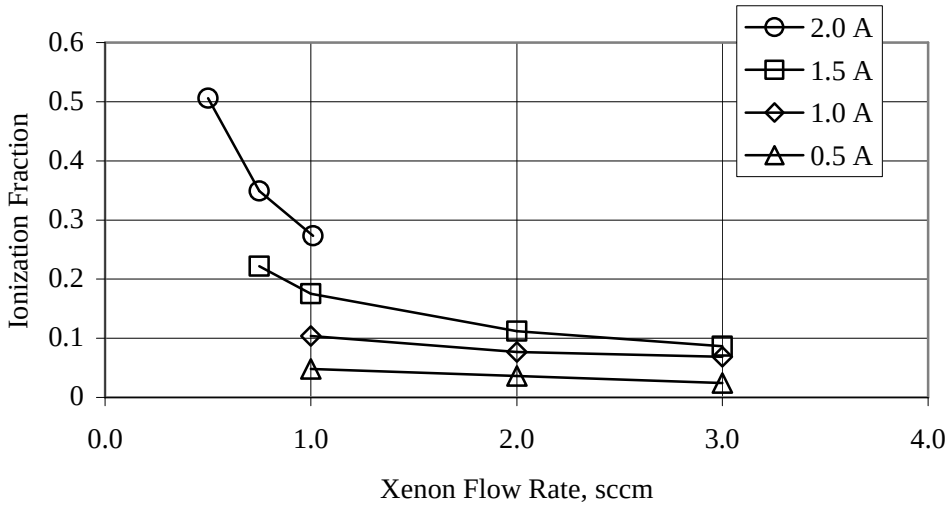

Figure 8 - Ionization fraction versus xenon flow rate for various cathode emission currents. Ion optics removed.

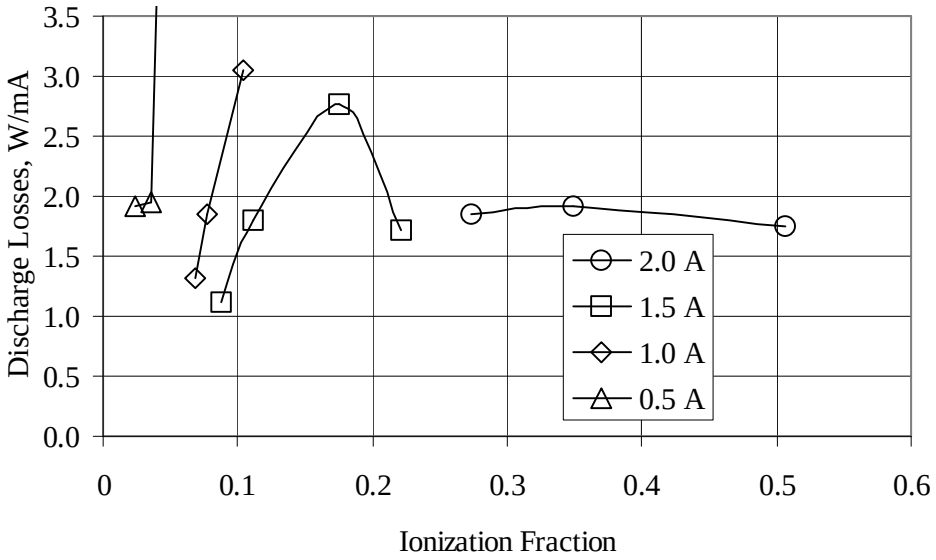

Figure 9 - Discharge losses versus xenon ionization fraction for various cathode emission currents. Ion optics removed.

Figure 10 - HCMT operation with beam extraction.

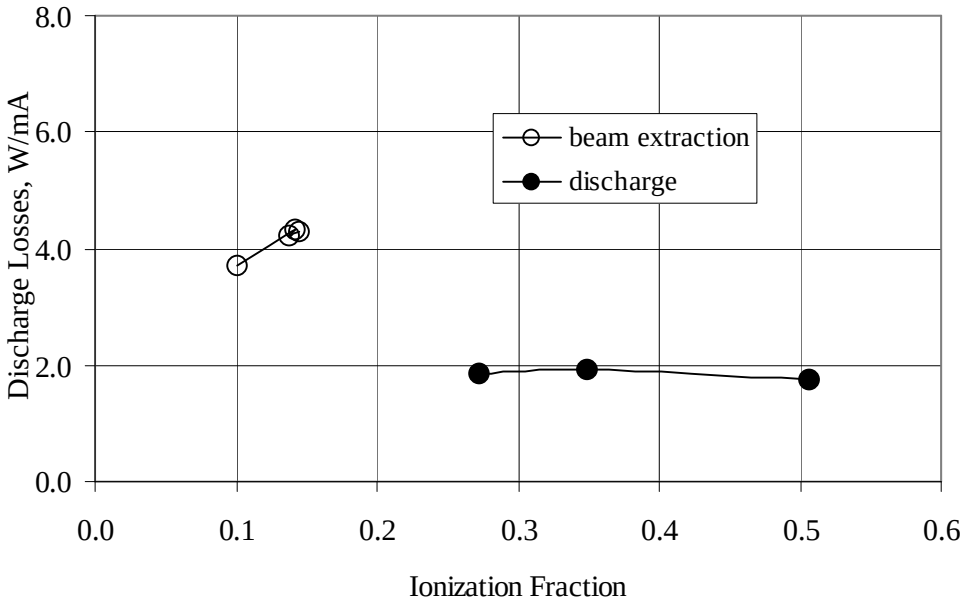

Figure 11 - Discharge losses versus xenon ionization fraction with and without beam extraction; 2.0 A cathode emission current.

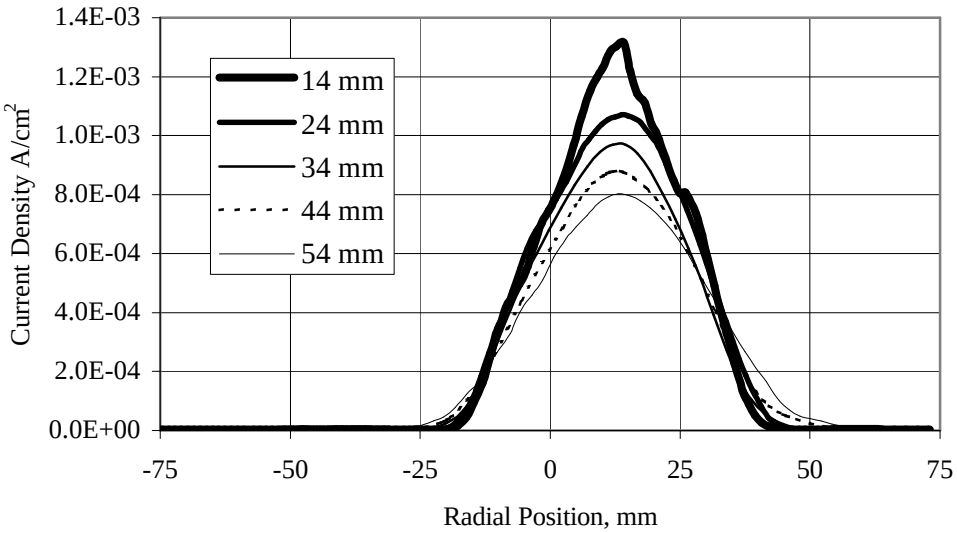

Figure 12 - Ion current density profiles at various axial distance.

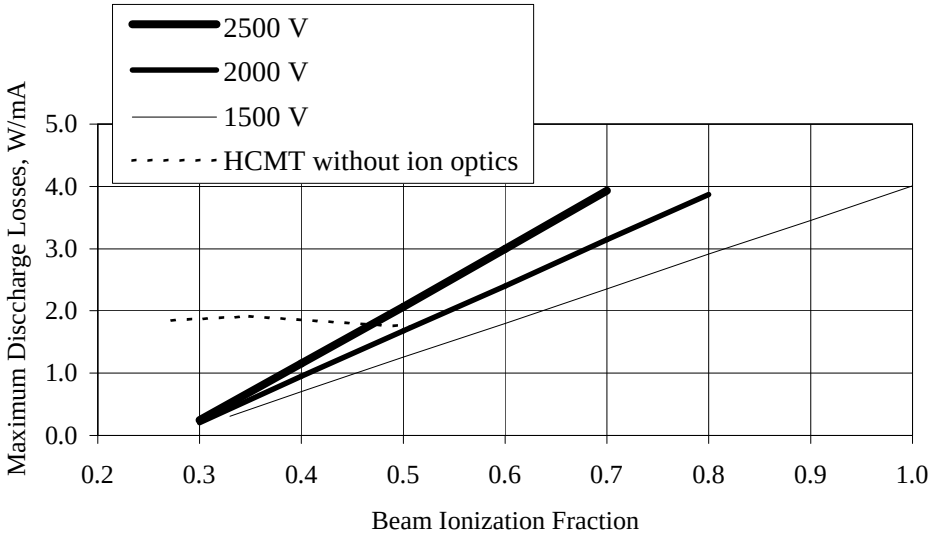

Figure 13 - Maximum acceptable discharge losses versus beam ionization fraction for various beam voltages; 25% engine efficiency, 7.74 mA beam current.